Viscoelastic Behavior of 1-Dodecanol Monolayers Undergoing a Liquid−Solid Phase Transition. A Surface Quasielastic Light Scattering Study

Mercedes G. Muñoz, Larisa Luna, Francisco Monroy, Ramón G. Rubio, and Francisco Ortega*

Departamento de Química Física I, Facultad de Ciencias Químicas, Universidad Complutense, E-28040 Madrid, Spain

Received February 3, 2000. In Final Form: April 5, 2000

A surface quasielastic light scattering (SQELS) and electrocapillary wave (ECW) study of a monolayer of 1-dodecanol, obtained by placing a reservoir drop of the alcohol on top of a water surface, has been carried out as a function of temperature at different wavevectors. This monolayer goes through a liquid−solid phase transition at 312.1 K, more than 14 K above the freezing of bulk 1-dodecanol. The fit of the SQELS spectra gives the frequency, ω_c, and the temporal damping, $\Delta\omega_c$, of thermally induced capillary waves. In all the temperature range ω_c follows Kelvin-like behavior (i.e., $\omega_c \sim q^{3/2}$) leading to values of the apparent dynamic surface tension lower than the static ones. In addition the damping follows, $\Delta\omega_c \sim q^{1.2-1.4}$ very far from the expected $\sim q^2$ dispersion behavior. Both wave parameters show temperature trends compatible with the expected liquid−solid 2D phase transition at around 312 K. The expansion of the frequency range by using the ECW technique, shows that our experimental results cover the regions $q \leq q_R \leq q$, where q_R is the wavevector at which capillary-dilational resonance takes place. Within the classical elasto-hydrodynamic theory, our results can be accounted for if the dilational viscosity, κ, takes a negative sign. In these conditions mode mixing takes place for $q \geq q_R$. Alternatively the experimental results can be quantitatively explained with $\kappa = 0$ if an extra hydrodynamic coupling is included in the dispersion equation. From a physicochemical point of view this coupling may arise from the vicinity of the phase transition and/or molecular orientational effects promoted by the dilational wave. The small values of the dynamic elasticity, $\epsilon(\omega)$, found in this work can be rationalized in terms of a monolayer−subsurface material transport, within the Lucassen−Van de Tempel model.

1. Introduction

Medium- and long-chain alcohols present high equilibrium spreading pressures and form stable monolayers on water; early works on monolayers of these chain alcohols have been summarized in the book by Gaines.[1] This monograph points out that experimental problems associated with evaporation of the alcohol, slow spreading and dissolution into the subphase, may be important issues in the study of these monolayers, mainly when the spreading is performed from solid particles of the alcohol.

In the past few years there has been a renewed interest in the study of chain alcohol monolayers, both from the theoretical[2] and the experimental sides.[3−9] Most of these studies have been carried out on monolayers formed by placing a reservoir drop of the alcohol on top of a clean water surface. This procedure leads to condensed monolayers at the equilibrium spreading pressure.

X-ray grazing incidence,[4−7,9] ellipsometry,[3,10] sum-frequency spectroscopy,[8,11] fluorescence,[12] and Brewster angle[13] microscopy and surface tension measurements[3,6,10,14] show that monolayers of medium- and long-chain alcohols ($C_nH_{2n+1}OH$; $n = 9-16$) present a 2D first-order liquid−solid phase transition upon decreasing temperature. For all the alcohols studied, this transition has been located more than 10 K above the melting temperature of the corresponding bulk phase. In this sense it is similar to the phenomenon of surface freezing recently observed in the free surface of *n*-alkanes[15−19] and hydrated long chain alcohols.[20−23] In these cases a solid 2D layer is formed on top of the bulk melt, but the temperature range for coexistence of the 2D solid and the bulk liquid is much smaller than in the case considered in the present work.

* To whom correspondence should be addressed. E-mail: Fortega@eucmax.sim.ucm.es.

(1) Gaines, G. L., Jr. *Insoluble Monolayers at Liquid−Gas Interfaces*; Interscience Pub., John Wiley & Sons: New York, 1966.
(2) Rieu, J. P.; Vallade, M. *J. Chem. Phys.* **1996**, *104*, 7729.
(3) Berge, B.; Renault, A. *Europhys Lett.* **1993**, *21*, 773.
(4) Renault, A. L.; J. F.; Goldmann, M.; Berge, B. *J. Phys. II* **1993**, *3*, 761.
(5) Legrand, J. F. R., A.; Konovalov, O.; Chevigny, E.; Als-Nielsen, J.; Grübel, G.; Berge, B. *Thin Solid Films* **1994**, *248*, 95.
(6) Berge, B.; Konovalov, O.; Lajzerowicz, J.; Renault, A.; Rieu, J. P.; Vallade, M. *Phys. Rev. Lett.* **1994**, *73*, 1652.
(7) Rieu, J. P. L., J. F.; Renault, A.; Berge, B.; Ocko, B. M.; Wu, X. Z.; Deutsch, M. *J. Phys. II* **1995**, *5*, 607.
(8) Casson, B. D.; Rüdiger, B.; Bain, C. D. *J. Chem. Soc., Faraday Discuss.* **1996**, *104*, 209.
(9) Zakri, C.; Renault, A.; Rieu, J. P.; Vallade, M.; Berge, B.; Legrand, J. F.; Vignault, G.; Grübel, G. *Phys. Rev. B* **1997**, *55*, 14163.
(10) Bonosi, F.; Renault, A.; Berge, B. *Langmuir* **1996**, *12*, 784.
(11) Casson, B. D.; Bain, C. D. *J. Phys. Chem. B* **1998**, *102*, 7434.
(12) Lenne, P. F.; Valance, A.; Bonosi, F.; Berge, B.; Misbah, C. *Europhys. Lett.* **1997**, *38*, 301.
(13) Overbeck, G. A.; Hönig, D.; Möbius, D. *Langmuir* **1993**, *9*, 555.
(14) Toyomasu, T.; Takiue, T.; Ikeda, N.; Aratono, M. *Langmuir* **1998**, *14*, 7313.
(15) Earnshaw, J. C.; Hughes, C. J. *Phys. Rev. A* **1992**, *46*, R4494.
(16) Hughes, C. J.; Earnshaw, J. C. *Phys. Rev. E* **1993**, *47*, 3485.
(17) Wu, X. Z. S., E. B.; Sinha, S. K.; Ocko, B. M.; Deutsch, M. *Phys. Rev. Lett.* **1993**, *70*, 958.
(18) Wu, X. Z. O., B. M.; Sirota, E. B.; Sinha, S. K.; Deutsch, M.; Cao, B. H.; Kim, M. W. *Science* **1993**, *261*, 1018.
(19) Sirota, E. B. *Langmuir* **1998**, *14*, 3133.
(20) Deutsch, M. W., X. Z.; Sirota, E. B.; Sinha, S. K.; Ocko, B. M.; Magnussen, O. M. *Europhys. Lett.* **1995**, *30*, 283.
(21) Sirota, E. B. W., X. Z. *J. Chem. Phys.* **1996**, *105*, 7763.
(22) Gang, O. O., B. M.; Wu, X. Z.; Sirota, E. B.; Deutsch, M. *Phys. Rev. Lett.* **1998**, *80*, 1264.
(23) Gang, O.; Wu, X. Z.; Ocko, B. M.; Sirota, E. B.; Deutsch, M. *Phys. Rev. E* **1998**, *58*, 6086.

10.1021/la0001474 CCC: $19.00
Published on Web 07/06/2000

The X-ray diffraction studies[4−7,9] suggest a solid-like hexatic structure below the transitional temperature T_f, with zero tilting of the molecules at the interface. However no Bragg diffraction is reported at $T > T_f$. This liquid−solid transition is accompanied by a collective tilting of the molecules at the interface.[8] On the theoretical side,[2] both molecular dynamics (MD) simulations and statistical models show evidence of a phase transition, which is identified with a 2D freezing of the alcohol monolayers. Furthermore, these works show that the conformational degrees of freedom play a fundamental role in the transition.

All the above-mentioned studies deal with static measurements, but unfortunately, information concerning the viscoelasticity of these monolayers is scarce. Earnshaw et al.[24] has studied the surface viscoelasticity of Gibbs monolayers of relatively soluble alcohols: 1-octanol and 1-decanol. One of the striking results of these surface quasielastic light-scattering (SQELS) experiments was the negative values of the dilational viscosity reported by these authors.

Negative dilational viscosities have been reported[25−29] in several other SQELS and electrocapillary wave (ECW) studies performed in both soluble and insoluble monolayers. A general understanding of these negative values of the dilational viscosity obtained within the currently accepted elasto-hydrodynamic theory[30] has not been reached yet.

Recent studies on the surface viscoelasticity of spread monolayers of insoluble fatty acids and esters seem to point out some kind of correlation of this unusual feature with the presence of a phase transitions in the monolayer.[29] Furthermore, Buzza et al.[31] have recently shown that under certain physical conditions, it would be necessary to take into account new contributions into the hydrodynamic description of the interface. Neglecting these contributions leads to effective viscoelastic coefficients, which might take physically unreasonable values.

Therefore, it seems necessary to elucidate from physical grounds the origin of this anomalous behavior, and its relation with the current hydrodynamic frame, used to obtain rheological information of 2D systems from propagation of surface modes.

In this paper, we present both SQELS and ECW experiments performed on a dense monolayer of 1-dodecanol on water in equilibrium with an excess drop of the bulk alcohol. This study has been carried out as a function of temperature in the liquid and the solid states of the monolayer and at different wavevectors in a broad q range ($10 < q/\mathrm{cm}^{-1} < 600$). Our aim is thus two-fold: on one side, to carry out a rheological study of the fluid−solid transition in a condensed monolayer, which has been well characterized from the structural point of view; on the other hand to compare the results obtained with those available for shorter (more soluble) alcohols.[24] This might allow us to obtain conclusions about the role of the phase behavior of the monolayer on its dynamics.

The rest of the paper is organized as follows: Section 2 provides a theoretical background on surface elasto-hydrodynamics. Section 3 contains experimental details and the description of the techniques. Section 4 presents the experimental results and section 5 its discussion. Finally, section 6 contains the main conclusions.

2. Theoretical Background

Liquid interfaces are in continuous motion due to the thermal fluctuations. This dynamic roughness is treated in terms of an infinite series of discrete Fourier modes each one characterized by a wavevector, q. In typical SQELS experiments the spanned length scale is 10^{-6} to 10^{-5} m, while the temporal one is typically in the kilohertz region. These limits are well inside the region in which a hydrodynamic approach can be safely used.[30,32] On the other hand, typical amplitude of these thermally excited modes is in the range of $10^{-9}-10^{-10}$ m; hence linear strain−stress relationships apply.[30,32]

From the classical theory, the hydrodynamic motion for a monolayer between two fluids can be decomposed in two main modes,[30,32,33] capillary (or out of plane) and longitudinal (or in plane). The capillary mode produces the strongest refractive index fluctuations, hence being mainly responsible for the observed scattered light intensity fluctuations.[32]

The capillary mode is essentially a shear motion, with surface tension, γ, and gravity, g, acting as restoring forces normal to the surface. The longitudinal motion can be decomposed in both, compression and shear contributions, characterized by two different elastic moduli (K and S, respectively). Since dissipative effects exist within the monolayer, each one of these uniaxial motions is governed by a set of viscoelastic response functions, which can be written as:[33,34]

$$\tilde{\gamma}(\omega) = \gamma + i\omega\mu \tag{1}$$

$$\tilde{\epsilon}_K(\omega) = K + i\omega\eta_K \tag{2}$$

$$\tilde{\epsilon}_S(\omega) = S + i\omega\eta_S \tag{3}$$

$$\tilde{\epsilon}(\omega) = \tilde{\epsilon}_K(\omega) + \tilde{\epsilon}_S(\omega) = \epsilon + i\omega\kappa \tag{4}$$

Equation 1 holds for the capillary motion and eq 3 for the longitudinal one, being ω the angular frequency. The imaginary parts of each of these viscoelastic moduli are the loss components related with viscous dissipation in the XZ plane (μ) and in the XY plane (η_K,η_S), XY being the plane of the surface. It is customary[30,34−36] to define a total longitudinal viscoelastic modulus as a sum of the compression and shear moduli, defined by a real part or dilational elasticity, ϵ, and a dissipative term or dilational viscosity, κ. The shear contribution, S, will be zero except for solid films, where the dislocations and defects may be effective in accumulating elastic energy.[37,38] Also, the shear contribution to the dilational viscosity, η_S, although generally nonzero, is several orders of magnitude smaller than the compression one, η_K, even for solid films.[39] The

(24) Earnshaw, J. C.; McLaughlin, A. C. *Prog. Colloid Polym. Sci.* **1989**, *79*, 155.
(25) Earnshaw, J. C.; McLaughlin, A. C. *Proc. R. Soc. London, Sect. A* **1993**, *440*, 519.
(26) Earnshaw, J. C.; McCoo, E. *Langmuir* **1995**, *11*, 1087.
(27) Sharpe, D.; Eastoe, J. *Langmuir* **1996**, *12*, 2303.
(28) Monroy, F.; Giermanska-Kahn, J.; Langevin, D. *Colloids Surf., A* **1998**, *143*, 251.
(29) Giermanska_Kahn, J.; Monroy, F.; Langevin, D. *Phys. Rev. E* **1999**, *60*, 7163.
(30) Kramer, L. *J. Chem. Phys.* **1971**, *55*, 2097.
(31) Buzza, D. M. A.; Jones, J. L.; McLeish, T. C. B.; Richards, R. W. *J. Chem. Phys.* **1998**, *109*, 5008.
(32) Langevin, D. *Light Scattering by Liquid Surfaces and Complementary Techniques*; Langevin, D., Ed.; Marcel Dekker: New York, 1992; Vol. 41.
(33) Kawaguchi, M. *Prog. Polym. Sci.* **1993**, *18*, 341.
(34) Goodrich, F. C. *Proc. R. Soc. London, Sect. A* **1981**, *374*, 341.
(35) Lucassen-Reynders, E. H.; Lucassen, J. *Adv. Colloid Interface Sci.* **1969**, *2*, 347.
(36) Baus, M.; Tejero, C. F. *J. Chem. Phys.* **1983**, *78*, 483.
(37) Landau, L. D. L., E. M. *The theory of Elasticity*; Pergamon Press: Oxford, 1986.
(38) Nelson, D. R.; Halperin, B. I. *Phys. Rev. B* **1979**, *19*, 2457.

importance of the transverse viscosity, μ, or even its existence has been a matter of controversy.[31,34] Recently, Kikuchi et al.[40,41] have experimentally pointed out zero μ values for the free surface of liquids, at least up to frequencies of 10 MHz. Only for very dense insoluble monolayers might the transverse viscosity be expected to give appreciable contributions.[32,42]

The calculation of the fluctuation spectrum for a monolayer has been frequently discussed in the literature.[32] The theoretical spectra for both capillary and dilational waves have been derived independently by Kramer[30] and Langevin and Bouchiat.[43] If we restrict ourselves to the capillary waves, the only ones that scatter an appreciable amount of light, the power spectrum is

$$P_q(\omega) = -\frac{2k_BT}{\omega}\,\mathrm{Im}\left[\frac{\tilde{\epsilon}q^2 + i\omega\eta(q+m)}{D(q,\omega)}\right] \qquad (5)$$

with η being the subphase viscosity and m the inverse capillary penetration length, which gives us a measurement of the damping of the surface velocity field in the liquid, and is given by

$$m = \sqrt[+]{q^2 + \frac{i\omega\rho}{\eta}} \qquad (6)$$

where $\sqrt[+]{\ }$ stands for $Re[m] > 0$ and where ρ is the density of the subphase.

The function $D(q,\omega)$ in the denominator of eq 5 corresponds to the dispersion equation, which relates the propagation characteristics of the surface modes to the constitutive parameters of the system

$$D(q,\omega) = [\eta\omega(q-m)]^2 + [\tilde{\epsilon}q^2 + i\eta\omega(q+m)]\left[\tilde{\gamma}q^2 + i\eta\omega(q+m) - \frac{\rho\omega^2}{q}\right] = 0 \qquad (7)$$

For a given q, this equation has two different nontrivial roots, $\tilde{\omega}_C$ and $\tilde{\omega}_D$; each one ($\tilde{\omega} = \omega + i\,\Delta\omega$), contains both, a real part, ω, or propagation frequency, and an imaginary part, $\Delta\omega$, accounting for the damping of the capillary (C) and dilational modes (D), respectively. Equation 7 points out that capillary and dilational motions are coupled together, this coupling being the mechanism allowing measurement of dilational viscoelasticity from the analysis of capillary wave spectra. This hydrodynamic coupling, mainly caused by the asymmetry of the bulk phases adjacent to the interface,[30,43] is maximum at resonance, i.e., when capillary and dilational waves propagate at close frequencies, $\omega_C \sim \omega_D$. This resonance generally occurs when the $\epsilon/\gamma \approx 0.16$ condition is fulfilled[32] and vanishes in the limit $m \rightarrow q$, which is found at very low frequencies or at very large subphase viscosities.[32]

When $\tilde{\epsilon} = 0$ and $\mu = 0$, eqs 5 and 7 simplify to the case of a free liquid surface. In these conditions and when $y = \gamma\rho/4\eta^2 q \gg 1$, the zero order solution of the dispersion equation (eq 7) is a quite good approximation for the propagation of the capillary mode:[32]

$$\tilde{\omega}_C^0 = \omega_C^0(q) + i\Delta\omega_C^0(q) \approx \sqrt{\frac{\gamma}{\rho}}\,q^{3/2} + i\,\frac{2\eta}{\rho}q^2 \qquad (8)$$

This limit corresponds to the bare surface of a low viscosity liquid, e.g., the air−water interface. In eq 8 the real part of the complex frequency, $\tilde{\omega}_C$, corresponds to the Kelvin−Lamb frequency and the imaginary part to the ideal temporal damping. This first-order approach for the dispersion behavior of capillary modes will be used as initial value input when we come to numerically solve eq 7 in section 5.

3. Experimental Section

1-Dodecanol is a Fluka product (purity better than 99.5%) and was used as received. Water was double distilled and deionized in a Milli-Q-RG system. Its resistivity was always higher than 18 MΩ cm^{-1}. A stainless steel cylindrical cell, with two optical quartz windows, was half-filled with water, and a drop of the alcohol (~20 μL) was placed on top of the water surface with a Hamilton syringe. The cell was left to equilibrate for 24 h prior to the measurements. The temperature control in the cell was carried out by passing thermostated water through a jacket in which the cell was enclosed. The temperature in the cell was measured with a Pt-100 probe previously calibrated. With this setup the temperature of the cell was maintained constant within ±0.01 deg over long time periods. Before the drop was added, the surface of the water subphase was cleaned by suction with a Pasteur pipet attached to a small electrical water pump, until the expected surface tension for pure water was obtained. Static surface tension measurements were performed with a Pt Wilhelmy plate attached to an electrobalance.

Our surface light scattering apparatus is similar to the one described by other groups,[32,44−47] and it has been described elsewhere.[42] In brief, a polarized intensity stabilized laser beam, produced by a 25 mW He−Ne laser, was spatially filtered to ensure a clean expanded Gaussian intensity profile. The beam passes through a diffraction grating and then a focusing lens, which forms a 1:1 image of the spot on the grating on top of the liquid surface. The light scattered by thermally excited capillary waves is mixed in the detector with each diffraction order reflected by the surface (heterodyne detection) which allows the selection of the wavevector, q. The output of the detector, a photomultiplier (Hamamatsu R1104), goes to a homemade high-pass electrical filter, to prevent for saturation of the electronics, and then to an amplifier/band-pass filter (SR 560), which accommodates the signal entry in a FFT spectrum analyzer (SR760). An alternative detection has been performed with a PAD circuit and an autocorrelator (NICOMP 170).

The instrumental resolution is limited by the finite size of the light spot at the detector; one collects light scattered from capillary modes that spans a range $q \pm \Delta q$ around a particular wavevector q, this being the main source of instrumental broadening,[32] $\Delta\omega_I$, which should be properly accounted for in order to obtain reliable values of the spectral half-width (or temporal damping) of the surface modes. In our case[42] the instrumental function can be accurately described by a Gaussian function, $G(\omega)$, with half-width, $\Delta\omega_I$, that can be approximated by[32]

$$\Delta\omega_I \approx \frac{3}{2}\,\omega_C\,\frac{\Delta q}{q} \qquad (9)$$

The observed spectrum is then a convolution between the theoretical spectrum and the instrumental function, $G(\omega)$

$$P(\omega) = \mathrm{FT}^{-1}\{\mathrm{FT}[P_q(\omega)]\mathrm{FT}[G(\omega)]\} \qquad (10)$$

where FT is the Fourier transform and FT^{-1} denotes its inverse transform. If $P_q(\omega)$ is approximated by a Lorentzian function, the convolution is a Voigt function.[32]

(39) Maru, H. C.; Wasan, D. T. *Chem. Eng. Sci.* **1979**, *34*, 1295.
(40) Kikuchi, H.; Sakai, K.; Takagi, K. *Jpn. J. Appl. Phys.* **1991**, *30*, L1668.
(41) Kikuchi, H.; Sakai, K.; Takagi, K. *Phys. Rev. B* **1994**, *49*, 3601.
(42) Monroy, F.; Ortega, F.; Rubio, R. G. *Phys. Rev. E* **1998**, *58*, 7629.
(43) Langevin, D.; Bouchiat, M. A. *C. R. Acad. Sci.* **1971**, *272B*, 1422.
(44) Earnshaw, J. C.; McGivern, R. C. *J. Phys. D*: *Appl. Phys.* **1987**, *20*, 82.
(45) Richards, R. W.; Rochford, B. R.; Taylor, M. R. *Macromolecules* **1996**, *29*, 1980.
(46) Dorshow, R. B.; Hajiloo, A.; Swofford, R. L. *J. Appl. Phys.* **1988**, *63*, 1265.
(47) Sano, M.; Kawaguchi, M.; Chen, Y.-L.; Skarlupka, R. J.; Chang, T.; Zografi, G.; Yu, H. *Rev. Sci. Instrum.* **1986**, *57*, 1158.

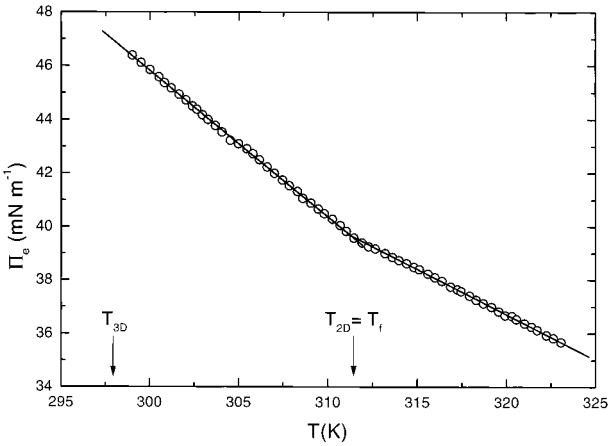

Figure 1. Experimental equilibrium spreading pressure, Π_e, as a function of temperature, T. The arrows indicate the location of the liquid−solid phase transition for the monolayer, $T_f = T_{2D}$, and the melting of bulk 1-dodecanol, T_{3D}. Lines are straight-line fits for $T > T_{2D}$ and $T < T_{2D}$.

The instrumental broadening produces a smearing out of the details of the spectra; as a consequence, to minimize the instrumental contribution is crucial. Our instrument has been calibrated using simple liquids (*n*-hexane, diethyl ether, and water); in particular diethyl ether and *n*-hexane both have very low viscosities, giving very large y values. In these conditions the surface spectrum is essentially Lorentzian and the width of the spectrum is mainly due to instrumental broadening, at low q values ($q < 900$ cm^{-1}). We have obtained an averaged value, $\Delta q = 6.2$ cm^{-1}, which corresponds to a very good resolution.[32,46]

The ECW setup is similar to that described by Ito et al.[48] and Stenvot et al.[49] In this technique surface capillary waves in the 20 Hz to 2 kHz range are excited at the air−liquid interface by ponderomotive effect, applying an ac electric field by means of a metal blade located within 0.1 mm of the interface. The spatial wavevector, q, and the corresponding wave damping coefficient, α, for these electrocapillary waves are determined by measuring the optical reflection of a laser beam focused at the interface. The phase difference and amplitude ratio between the applied field and the transverse deformation are measured as a function of the distance from the blade, avoiding one to obtain the propagation parameters q and α at a given frequency, ω. These propagation parameters are then used to obtain the elasticity modulus and dilational viscosity from the dispersion equation. So far, our experimental setup is restricted to work at room temperature. The instrument has been calibrated with water.

4. Results

Equilibrium Behavior. When a drop of 1-dodecanol is placed on top of a clean water surface, it spreads spontaneously over the surface giving a dense monolayer in equilibrium with the excess bulk material. In these conditions the measured surface tension, γ, corresponds to the so-called equilibrium spreading pressure (ESP), $\Pi_e = \gamma_0 - \gamma$, γ_0 being the surface tension of pure water. The experimental values of Π_e obtained for monolayers of 1-dodecanol in equilibrium with an excess drop are plotted in Figure 1 as a function of temperature. The melting point of 1-dodecanol in the bulk state is 294.25 K[23] and 296.55 K when hydrated;[23] all the data reported here correspond thus to the region in which the reservoir drop is in the liquid state. As can be seen, $d\Pi_e/dT$ presents a discontinuity at $T_f = 312.1$ K, in agreement with the results reported by other authors.[6,14] T_f corresponds to the freezing temperature for the 2D liquid−solid phase transition taking place in the monolayer. $\Delta S = d\Pi_e/dT$ accounts[1] for the change in entropy per unit area on spreading the film material from the 3D liquid drop (or from the crystalline particles). It is negative both above ($\Delta S_L = -0.339$ mN m^{-1} K^{-1}) and below ($\Delta S_S = -0.545$ mN m^{-1} K^{-1}) T_f. This, as expected, reflects the fact that in both cases the alcohol in the monolayer is in a more ordered state than in the liquid drop. The observed sequence in entropy decreasing corresponds, thus, first to the 2D confinement on going from the drop (3D liquid) to the liquid monolayer and then to the 2D ordered solid. However, if spreading takes place from the 3D solid state (from solid crystalline particles), an entropy increase ($\Delta S = d\Pi_e/dT > 0$) is observed since a large amount of long-range positional order is lost through one spatial dimension.[1] Only in this case is an increase of Π_e with temperature possible, as expected for Langmuir monolayers in the condensed state.

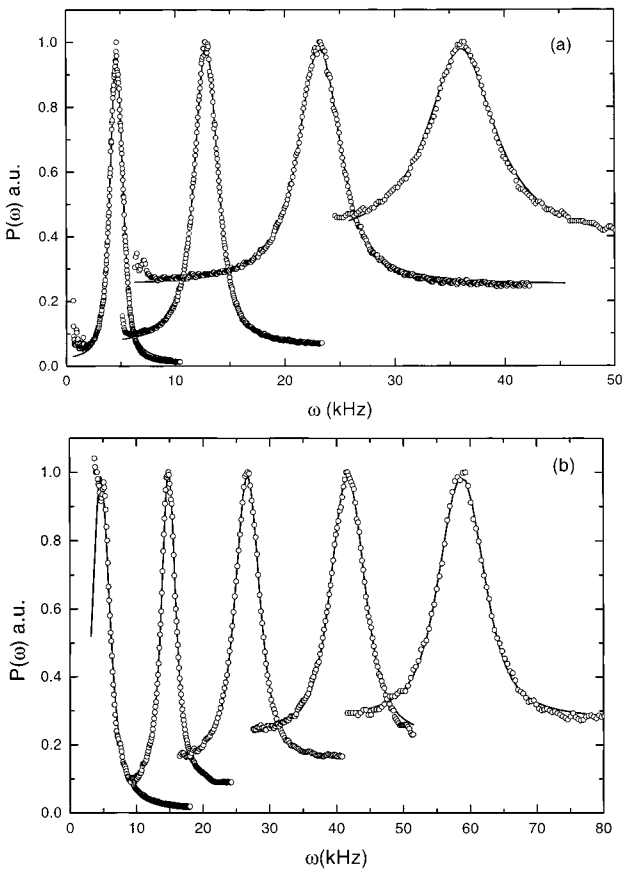

Figure 2. Experimental power spectra (a) obtained in the solid phase, $T = 298.45$ K. From left to right peaks correspond to wavevectors 99.5, 201.9, 316.2, and 404.9 cm^{-1}. (b) Obtained in the liquid phase, $T = 323.92$ K. From left to right peaks correspond to wavevectors 99.5, 201.9, 316.2, 404.9, and 510.7 cm^{-1}.

SQELS Results. We have measured the power spectra for the monolayers of 1-dodecanol at five different wavevectors from 99.5 to 510.7 cm^{-1} and at 19 temperatures ranging from 298.45 to 323.92 K. Figure 2 shows some experimental spectra at two temperatures near the edges of the temperature range; the quality of the spectra was similar at all the temperatures.

The analysis in terms of a Voigt function (see eq 10) (solid lines in Figure 2) gives the frequency, ω_C, and the half-width or damping, $\Delta\omega_C$, of the selected capillary mode together with the half-width of the Gaussian function, $\Delta\omega_I$, that accounts for the instrumental broadening. The experimental frequencies, ω_C, and half-widths, $\Delta\omega_C$, obtained at five different wavevectors are plotted as a function of the temperature in Figures 3 and 4, respec-

(48) Ito, K.; Sauer, B. B.; Skarlupka, R. J.; Sano, M.; Yu, H. *Langmuir* **1990**, *6*, 1379.
(49) Stenvot, C.; Langevin, D. *Langmuir* **1988**, *4*, 1179.

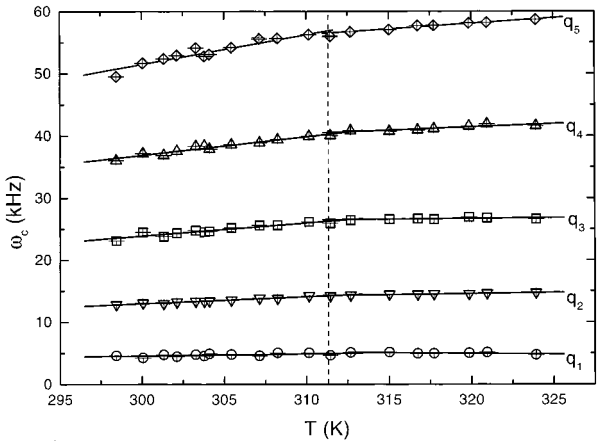

Figure 3. Capillary wave frequencies as a function of temperature for different wavevectors $q_1 = 99.5\ cm^{-1}$, $q_2 = 201.9\ cm^{-1}$, $q_3 = 316.2\ cm^{-1}$, $q_4 = 404.9\ cm^{-1}$, and $q_5 = 510.7\ cm^{-1}$. Solid lines correspond to the best straight-line fits for the liquid ($T > T_f$) and solid ($T < T_f$) regions. The vertical dash line corresponds to the transition temperature, T_f.

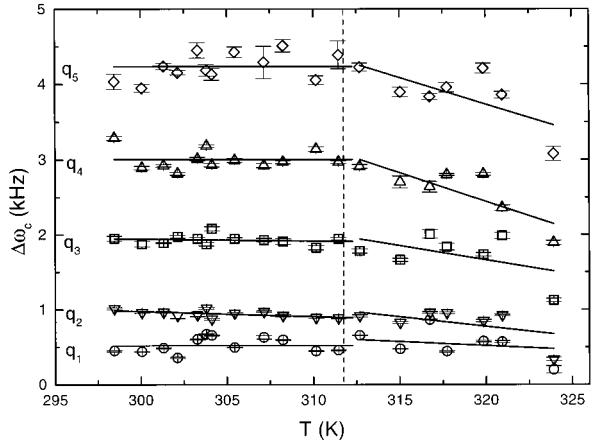

Figure 4. Capillary wave half-widths as a function of temperature for the same wavevectors as in the preceding figure. Solid and dash lines as in Figure 3.

tively. Each value reported here represents the average of at least two independent determinations.

Although the phase transition is observed at all the q values, it is more evident at higher wavevectors. This reflects the fact that the transverse stress, mainly governed by surface tension (the $d\gamma/dT$ derivative changes at T_f), is proportional[30] to γq^2, thus being the dispersion of the capillary mode more influenced by transitional effects at higher q. Both ω_C and $\Delta\omega_C$ are continuous through the transition, although the slopes of the log−log representations are different in the liquid side than from the solid one. Earnshaw[15,16] found discontinuities in both quantities for the surface freezing of fluid alkanes. The discontinuities were more evident at the higher q values. Above the transition temperature, the behavior found by Earnshaw is compatible with an alkane-free surface without any monolayer on top. When these results are compared with the present ones, the first thing that should be considered is that in our case both static surface tension and the capillary wave propagative parameters are compatible with the presence of a monolayer throughout all the studied temperature interval. Then we do not expect to find a discontinuity in ω_C or $\Delta\omega_C$, at the transition. Second, for $T < T_f$ Earnshaw's results show frequencies which decrease on decreasing temperature and half-widths which remain essentially constant, which is compatible with our results (see Figures 3 and 4).

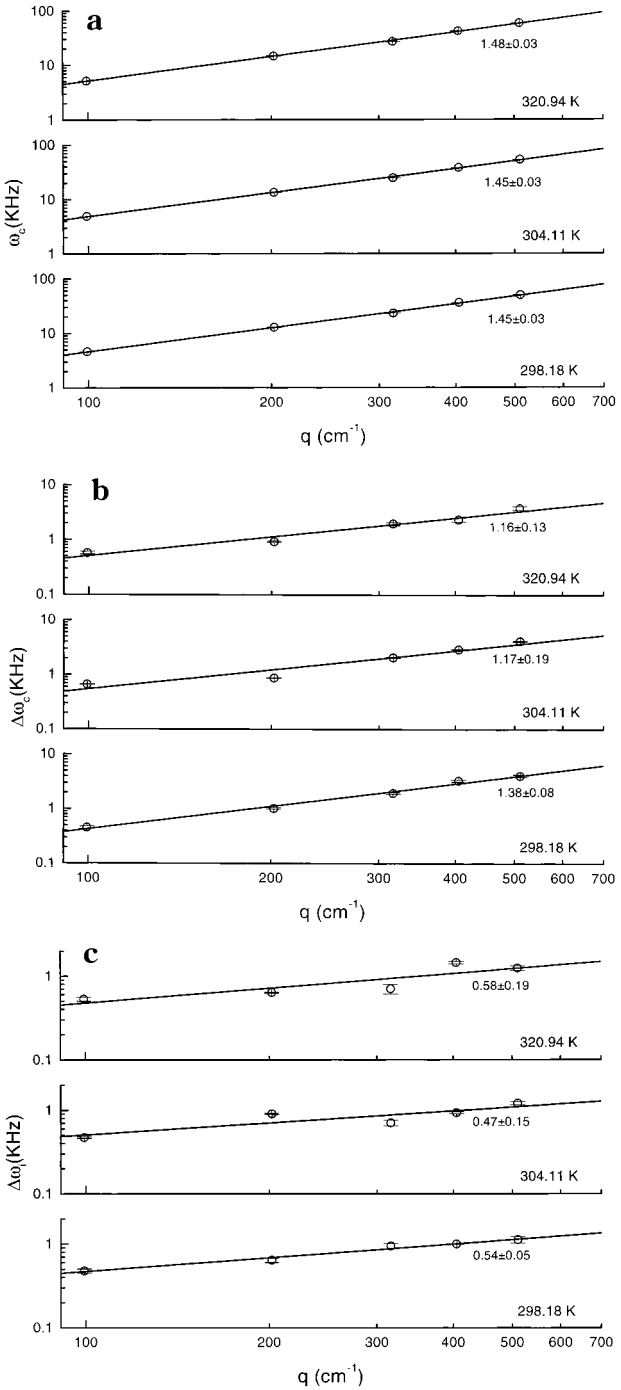

Figure 5. Frequencies, ω_c (a), half-widths, $\Delta\omega_c$ (b), and instrumental half-widths, $\Delta\omega_I$ (c), as a function of the wavevector for three temperatures. Solid lines correspond to the best straight-line fits with slopes indicated in the plot.

Figure 5 shows the values of ω_C, $\Delta\omega_C$, and $\Delta\omega_I$ that best fit the experimental spectra. They are represented as a function of wavevector for three selected temperatures. Similar results have been found for the rest of the temperatures.

As can be observed in Figure 5a, the *q-dependence of* ω_C is close to the one expected for the limiting Kelvin−Lamb ($\sim q^{3/2}$) behavior (see eq 8) characteristic of a simple liquid surface when $y \gg 1$. As a first-order approximation, we have obtained the apparent dynamic surface tensions, γ_d, by fitting the *q-dependence of* ω_C to eq 8. Figure 6 shows γ_d as a function of temperature, and for the sake of comparison we have replotted the equilibrium surface tension, γ. As can be observed, γ is always larger than γ_d

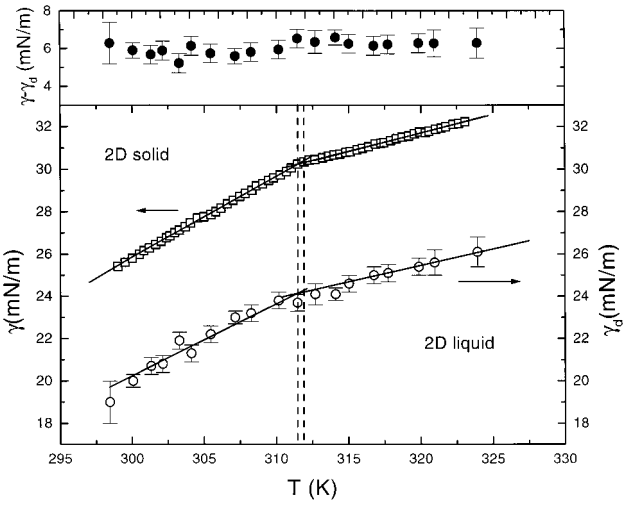

Figure 6. Static surface tension, γ (□), and apparent dynamic surface tension, γ_d (○), as a function of temperature, T. In the top of the figure is plotted the difference between γ and γ_d (●). Solid lines correspond to best straight-line fits for the liquid ($T > T_f$) and solid ($T < T_f$) regions.

by ca. 6 mN/m, which is a signature of the presence of a monolayer in the whole temperature range.[32,50] At T_f = 312.2 K there is a discontinuity in $d\gamma_d/dT$, indicating the phase transition: this value agrees well with the value of T_f obtained from the static results. It is worth mentioning that the constancy of $\gamma_d - \gamma$, with the temperature is a first indication of an unexpected result: in effect, for a monolayer, the capillary wave frequency is essentially determined[30] by the values of γ and ϵ, thus our results indicate that the difference in dilational elasticity between the 2D liquid and the solid is small.

From the hydrodynamic point of view, an interesting result is that the experimental values of the exponents of the q-dependence of $\Delta\omega_C$ (see Figure 5b) are between 1 and 1.4 over the whole temperature range. As already mentioned, these values are very different from the expected ideal damping dependence ($\Delta\omega_C \sim q^2$). When a monolayer is present there is a strong increase in the capillary wave damping in comparison with that for the free surface of the subphase; this is our case as can be seen by an inspection of the half-widths of the spectra (see Figure 2). Nevertheless, even under conditions of strong damping, the q-power of the capillary damping reported for a monolayer spread on a simple liquid are not far from the ideal value ($\sim q^2$),[26,32,42,50] in contrast with the present results. Furthermore, some of our experimental values show q-dependences close to the one that will be expected for pure dilational waves ($\sim q^{4/3}$).

As it can be observed in Figure 5c, the instrumental half-widths follow the expected trend, given by eq 9, with the value of Δq obtained from the calibration with simple liquids (see Section 3).

ECW Results. To extend the frequency range of our study, we have carried out ECW experiments. As already said, with this technique it was only possible to measure at room temperature: 296.1 K. This temperature is lower than T_f, and so the experiment was performed on the solid phase of the monolayer. Figure 7a shows the q-dependence of the frequency of the electrocapillary waves together with those of the thermally excited waves (SQELS); the agreement is good despite the fact that the experiments are not performed at exactly the same temperature. In

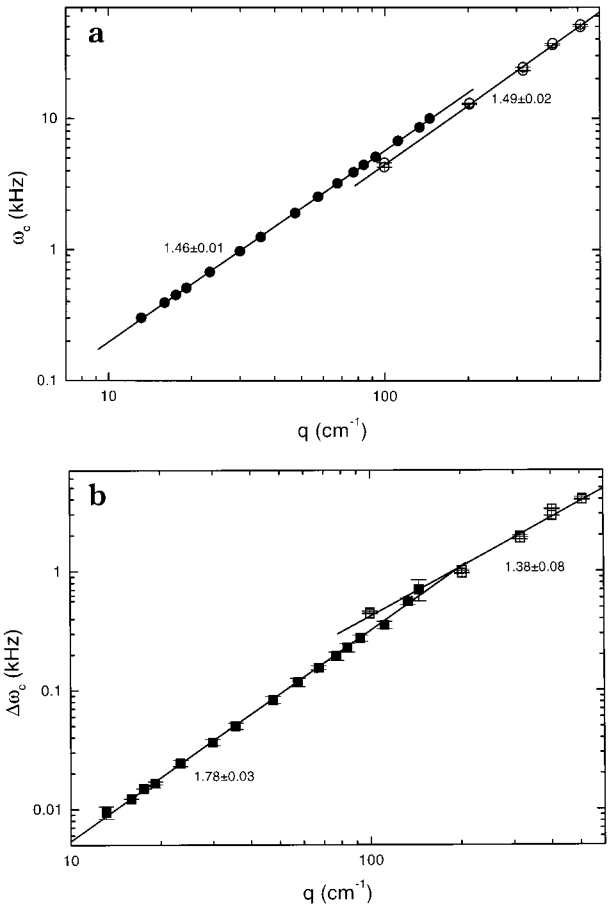

Figure 7. (a) Experimental ECW frequencies (●) and SQELS frequencies (○) as a function of the wavevector, q. ECW data correspond to a temperature of 296.1 K and SQELS to 298.4 K. The solid line corresponds to the best straight-line fits to both ECW and SQELS sets of data with slopes as indicated. (b) Experimental ECW (■) and SQELS (□) damping as a function of the wavevector, q, for the same temperatures as before. Solid lines correspond to the best straight-line fits to both sets of data with slopes indicated in the graph.

both cases, the slopes are close to the ideal value given by the Kelvin law (1.5). The shift in the q scale between both type of measurements (≈10%) is due to the difference in temperature and thus in surface tension. The damping of the capillary mode is plotted in Figure 7b as a function of wavevector. The spatial damping data, α_C, obtained from ECW must be transformed to equivalent temporal damping, $\Delta\omega_C$, to compare them with the SQELS results. This can be done through the group velocity,[51] $U = \partial\omega/\partial q$, which leads to $\Delta\omega_C = U\alpha_C$. Despite the above-mentioned q-shift, Figure 7b clearly shows that around 100 cm^{-1} there is a change in the slope from a value of 1.8 (close to the one expected for pure capillary waves) to a value of 1.4, close to what should be obtained for a pure dilational wave (at higher temperatures the slope is even smaller, see Figure 5b). Since the capillary mode for a viscoelastic monolayer at the air−water interface is usually damped as $\sim q^2$, this is a result which deserves explanation from a hydrodynamic point of view.

5. Discussion

Viscoelasticity. Using the equilibrium surface tension and the experimental ω_C and $\Delta\omega_C$ data, the dynamical values of the dilational elasticity, $\epsilon(\omega)$, and viscosity, $\kappa(\omega)$,

(50) Kolevzon, V.; Pozdniakov, G. *J. Phys.: Condens. Matter* **1997**, *9*, 6815.

(51) Lamb, H. *Hydrodynamics*; Dover: New York, 1945.

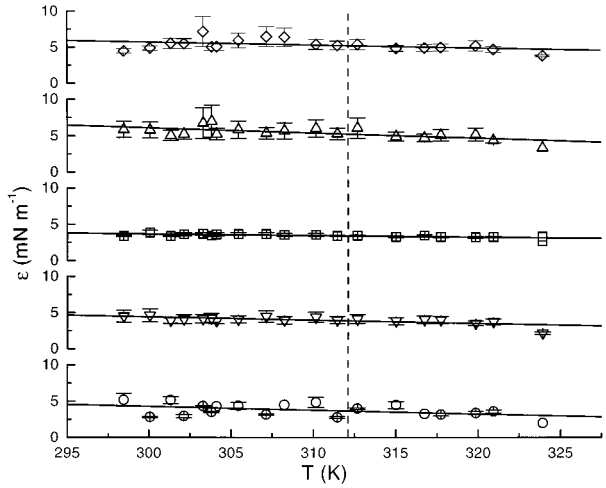

Figure 8. Calculated dilational elasticities, ϵ, as a function of temperature, for different wavevectors. Solid lines are only eye guides and vertical dash line corresponds to the transition temperature, T_t. Wavevector values as in Figure 3.

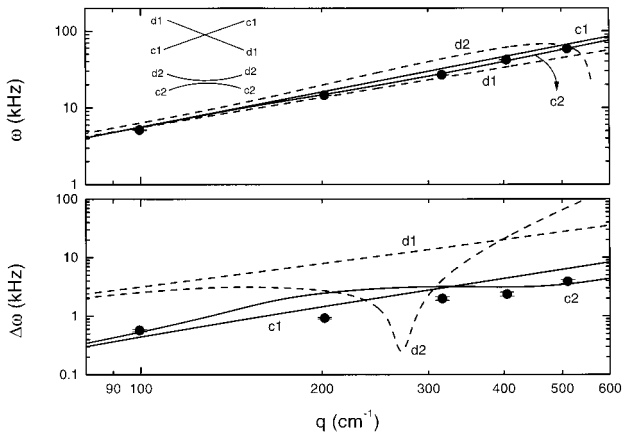

Figure 9. Capillary (c, solid lines) and dilational (d, dash lines) frequencies (ω) and damping ($\Delta\omega$) calculated from the dispersion equation (eq 7) for $T = 320.94$ K, $\gamma = 31.8$ mN m^{-1} and $\epsilon = 4$ mN m^{-1} with (c1, d1) $\kappa = 0$ and (c2, d2) $\kappa = -1.2\ 10^{-7}$ kg s^{-1}. (●) Experimental SQELS data for the same temperature.

have been obtained by solving the classical dispersion equation (eq 7). Following Buzza et al.[31] we have neglected the transverse viscosity, μ (see also discussion below, section 5, SQELS spectra). The calculated elasticities are small, within 3 and 6 mN m^{-1}, and κ is negative ranging from -1×10^{-7} to -2×10^{-7} kg s^{-1} for all the temperatures and wavevectors. The values of $\epsilon(\omega)$ are plotted in Figure 8 as a function of temperature, for the different wavevectors. Note that, at least in the frequency range considered here, $\epsilon(\omega)$ is continuous through the transition within the experimental precision.

The viscoelastic results reported here for dense monolayers of 1-dodecanol are in good agreement with the rheological behavior previously reported for adsorbed monolayers of shorter 1-alcohols. Earnshaw et al.[24] have carried out QESLS experiments on monolayers of 1-decanol and 1-octanol, and Sharpe et al.[27] have also studied this last system. The values of the dilational viscosity found by these authors ($\kappa \sim -1\ 10^{-7}$ kg s^{-1}) are in agreement with the ones we report here. When comparing the loss modulus, $\omega\kappa$, obtained at different frequency domains (SQELS or ECW methods) and from systems with different chemical nature, e.g., adsorbed monolayers of ionic[26-28] and nonionic surfactants[27] or spread monolayers of fatty acids,[29] values ranging between -10 and -30 mN m^{-1} are found in these systems which exhibit *anomalous* dilational viscosity. Moreover, in general, $\omega\kappa$ is almost always found to be nearly independent of the frequency. Concerning the values of the dilational elasticity modulus, we have reported here $\epsilon \sim 3-6$ mN m^{-1} for frequencies in the kilohertz domain, while Earnshaw et al.[24] reported, at similar frequencies, $\epsilon \sim 35$ mN m^{-1} for absorbed monolayers of 1-decanol and a value slightly larger, $\epsilon \sim 45$ mN m^{-1}, for 1-octanol; we will come back to this point in the final section.

Now let us examine two key questions that remain yet unexplained: Which is the meaning of the negative values obtained for the dilational viscosity coefficient, $\kappa(\omega)$? Does it quantitatively affect the calculated values of the dilational elastic modulus, $\epsilon(\omega)$? As it will be pointed out in the next paragraph, some of these questions may be partially clarified from the analysis of the dispersion behavior of the surface modes.

Dispersion Behavior. The fact that eq 7 gives negative values of κ is directly related with the $\Delta\omega_c$ values and their dependence with q. To understand these results, we have to look in detail to the solutions of the dispersion equation. Equation 7 has two different nontrivial roots corresponding to the two surface modes; if $\epsilon \gg \gamma$ or $\epsilon \ll \gamma$ (uncoupled state), each mode can be considered as a pure capillary or dilational wave and is characterized by the corresponding complex frequencies, $\tilde{\omega}_C$ ($=\omega_C + i\Delta\omega_C$) and $\tilde{\omega}_D$ ($=\omega_D + i\Delta\omega_D$), respectively. The zero order approximation ($y \gg 1$, $\epsilon = 0$) for $\tilde{\omega}_C$ is given by eq 8, and similarly when γ is set to zero the dilational mode follows, when $y \gg 1$:

$$\tilde{\omega}_D = \frac{1}{2}(\sqrt{3} + i)\left(\frac{\tilde{\epsilon}^4 q^4}{\eta\rho}\right)^{1/3} \tag{11}$$

When both γ and ϵ are nonzero, coupling between capillary and dilational modes occurs. This coupling is a maximum close to the resonance condition $\omega_C = \omega_D = \omega_R$, when both frequencies (eq 8 and eq 11) coincide at a wavevector:

$$q_R = \left(\frac{3}{4}\right)^3 \frac{\epsilon^4 \rho}{\gamma^3 \eta^2} \tag{12}$$

Let's assume that the values obtained for $\epsilon(\omega)$ by solving eq 7 ($\epsilon(\omega) \sim 3-6$ mN m^{-1}) are correct, thus eq 12 gives q_R values between 30 and 500 cm^{-1}. This means that most of our SQELS data lie in a q range close to or above the resonance condition, while the ECW data correspond to $q \leq q_R$. Therefore it is necessary to discuss the effect of resonance in the dispersion of the capillary waves. Figure 9 shows the q-dependence of the frequency and damping, corresponding to both capillary and dilational modes, as obtained by solving numerically the dispersion equation (eq 7). For the sake of clarity this figure shows only the SQELS data corresponding to one experimental temperature in the 2D solid phase ($T = 320.94$ K, $\gamma = 31.8$ mN m^{-1} and $\epsilon = 4$ mN m^{-1}). Similar results have been found for the rest of the temperatures studied. By setting $\kappa = 0$ in the dispersion equation, the calculated values of the dilational and capillary frequencies crossover at $q = q_R \approx 100$ cm^{-1} (resonance), but the effect on the capillary damping is hardly observed. When κ is decreased below a threshold negative value, κ_c, the effect is, however, completely different: Figure 9 shows that ω_C and ω_D no longer crossover, but they approach each other until a wavevector near to q_R and then separate out. For $q > q_R$ the damping of both modes changes abruptly, and the dispersion behavior cannot be easily assigned to a pure

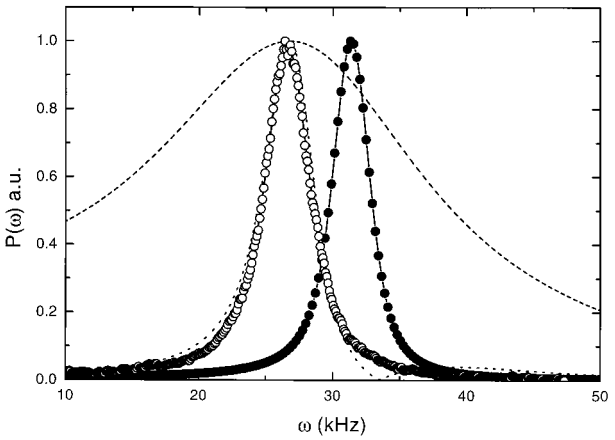

Figure 10. Experimental power spectrum for a wavector 316.2 cm^{-1} and a temperature 315.02 K (○): solid line, the best fit to a Voigt function; dash line, theoretical spectrum (eq 5, eq 10) with $\epsilon = 0$, $\kappa = 0$, $\mu = 5 \times 10^{-7}$ kg s^{-1}, and $\Delta q = 6.2$ cm^{-1}; dot line, theoretical spectrum with $\epsilon = 3.3$ mN m^{-1}, $\kappa = -1.6 \times 10^{-7}$ kg s^{-1}, and $\mu = 0$. Experimental power spectrum (●) for a free water surface in the same conditions, solid line corresponds to the best fit to eq 10 with the theoretical spectrum (eq 5, eq 10, $\epsilon = 0$, $\kappa = 0$, $\mu = 0$, and $\Delta q = 6.2$ cm^{-1}).

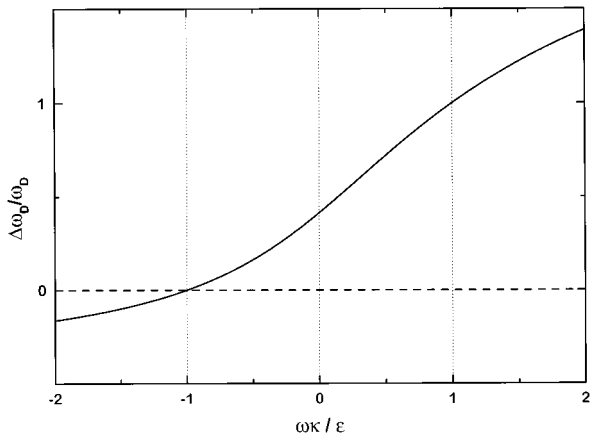

Figure 11. Dispersion behavior for the dilational mode. Dimensionless damping−frequency ratio as a function of the dimensionless loss module−elasticity ratio.

capillary or dilational wave. This behavior is due to linear mode mixing,[25] Earnshaw et al.[52] found a similar behavior for $\kappa = 0$ when μ is increased above a threshold value, μ_c, establishing two different and equivalent ways for hydrodynamic mode mixing at a frequency close to resonance: either, negative values of the dilational viscosity coefficient, $\kappa < 0$, or positive and large, transverse viscosity, $\mu \gg 0$, both leading to an abnormally high capillary damping (much larger than the one expected for a purely elastic surface).

Mode mixing (obtained by setting $\mu > \mu_c$ or $-\kappa > -\kappa_c$) is able to qualitatively explain our experimental results concerning the slopes of the capillary damping $\Delta\omega$ against q. Near and above the resonance condition (SQELS results) the experiments probe a transverse mode which damping is dispersed as that corresponding to the dilational mode, i.e., $\Delta\omega \sim q^{4/3}$. Far form the resonance condition, $q \ll q_R$ (ECW results), mode mixing is largely prevented and the transverse motion is damped as a near-pure capillary mode, $\Delta\omega \sim q^2$.

On the other hand, eq 12 points out a strong dependence of q_R on the dilational elasticity modulus ($\sim\epsilon^4$), which can be used to calculate a reasonably accurate value of the elasticity of the system if resonance is clearly observed from the dispersion behavior. From the experimental results in Figure 7b a clear near-to-resonance condition followed by mode mixing ($\kappa < 0 \rightarrow \Delta\omega \sim q^{4/3}$) is observed at $q_R \sim 100-200$ cm^{-1}, leading to $\epsilon \sim 4-5$ mN m^{-1}, as already calculated by solving the dispersion equation. Since the condition for resonance is not sensible to dissipation effects,[35,52] this estimation is particularly useful in order to confirm the validity of the values of the elasticity modulus, notwithstanding the effect of negative dilational viscosity.

Mode Mixing from $\kappa < 0$ or $\mu \gg 0$. Analysis of the SQELS Spectra. Fitting the experimental spectra to eq 10 allows us to distinguish between the two scenarios for mode mixing ($\kappa < 0$ or $\mu \gg 0$). Figure 10 shows that it is not possible to reproduce our experimental spectra if ϵ and κ are constrained to be positive for any value of μ. In effect, assuming $\mu = 0$, the frequency of the maximum given by the theoretical spectrum is always higher than the experimental one and close to the values corresponding to a free water surface ($\epsilon = 0$ and $\kappa = 0$, in Figure 10) for any values of ϵ and $\kappa > 0$. The experimental values of ω_c can be obtained by increasing μ to an unreasonable value of 5 10^{-7} kg s^{-1}, (Figure 10). However in this case the spectral width is exceedingly high compared to the experimental one, this result being almost independent of the chosen ϵ and κ values. If κ is not constrained to be positive, a good approximation for both maximum frequency and shape can be obtained (see Figure 8), although the theoretical spectrum shows a small bump at the high-frequency side which has not been observed experimentally. As can be seen in Figure 10, the best fit is obtained assuming a Lorentzian spectral shape (Voigt function).

Therefore it seems clear from the analysis of the spectra that, at least for the present system, $\kappa < 0$ instead of $\mu \gg 0$ should be chosen in order to reach mode mixing.

An Alternative Dispersion Equation. The negative values of the dilational viscosity may be interpreted in terms of an energy transfer to the dilational mode from other surface modes. It must be emphasized that $\kappa < 0$ does not necessarily imply hydrodynamic instability[53,54] of the dilational mode in the sense of a negative damping, which is only expected for a system far from equilibrium. In fact, using eq 11 we have plotted the dependence of the reduced damping $\Delta\omega_d/\omega_d$ of the dilational wave as a function of the $\omega\kappa/\epsilon$ ratio (Figure 11). It is clear, from the graph, that the dilational mode exhibits viscous losses even for $\kappa = 0$, arising from the coupling to the capillary mode. However dilational instability ($\Delta\omega/\omega < 0$) does not appear until $\kappa < -\epsilon/\omega$.

We have already explained that from the point of view of hydrodynamics *effective* negative values of κ indicate an extra coupling between the dilational mode and the capillary one, or with other mode not explicitly considered in the classical dispersion equation (see eq 7). To explore empirically this possibility, we will make use of the dispersion equation proposed recently by Buzza et al.[31] These authors have included the bending mode in the hydrodynamic description of thick monolayers made of copolymers at the air−water interface. The dispersion equation also includes a coupling term between the bending, which is a transverse motion, and the capillary-dilational modes. Although, strictly speaking, these terms

(52) Earnshaw, J. C.; McLaughlin, A. C. *Proc. R. Soc. London, Sect. A* **1991**, *433*, 663.

(53) Hennenberg, M.; Chu, X.-L.; Sanfeld, A.; Velarde, M. G. *J. Colloid Interface Sci.* **1992**, *150*, 7.

(54) Noskov, B. A.; Loglio, G. *Colloids Surf., A: Physicochem. Eng. Aspects* **1998**, *143*, 167.

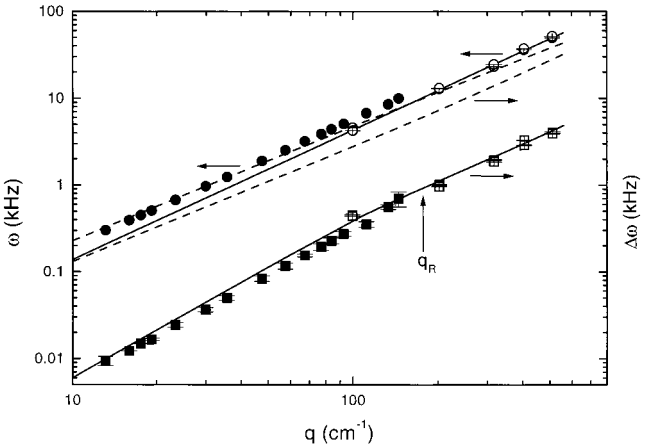

Figure 12. Capillary (—) and dilational (- - -) frequency (ω) and damping ($\Delta\omega$) calculated from eq 13 for $T = 298.4$ K, $\epsilon = 4.0$ mN m^{-1}, $\kappa = \mu = 0$ and $\lambda = 2.4 \times 10^{-5}$ mN. Experimental SQELS and ECW data are the same as in Figure 7.

should not be important for thin monolayers, we have considered it interesting to explore the effect that a term like the coupling one of Buzza et al. might have on the results. This may be considered as an *ad hoc* change of the classical dispersion equation (eq 7) that includes a supplementary reaction term between the dilational-capillary modes and another hydrodynamic mode that, by itself, does not lead to significant scattering of light. In Buzza's theoretical treatment the coupling constant, λ, is a constitutive parameter of the interface and, in addition to the classical coupling due to the asymmetry of the bulk phases defining the interface, directly couples surface normal displacements to the tangential restoring forces controlled by the elasticity and tangential displacements to the normal restoring force, controlled by the surface tension. A simplified version of the dispersion equation obtained from this treatment, neglecting only the bending contribution and not the coupling term, is the following

$$D(q,\omega) = [\eta\omega(q - m) + i\lambda q^3]^2 + [\tilde{\epsilon}q^2 + i\eta\omega(q + m)] \times \left[\tilde{\gamma}q^2 + i\eta\omega(q + m) - \frac{\rho\omega^2}{q}\right] = 0 \quad (13)$$

which reduces to eq 7 when there is no coupling, $\lambda = 0$.

Using this dispersion equation, we can quantitatively explain all our experimental data. The resulting values of ϵ are equal, within the experimental error, to the ones obtained with eq 7 ($\lambda = 0$), and the data can be fitted using an almost constant value of the coupling constant, λ ($2-3 \times 10^{-5}$ mN), and $\mu = \kappa = 0$. Figure 12 shows the fit for the same results as in Figure 7. As can be observed, eq 13 predicts the same crossing of dilational and capillary frequencies at q_R as eq 7 does for small κ values. The dilational damping is now an order of magnitude larger than the capillary one for all q and is not practically affected by the resonance.

Although it is difficult to explain a high value of λ for this thin monolayer, it seems that the inclusion of a coupling term produces a crossover of the capillary damping from a capillary-like dependence ($\Delta\omega \sim q^2$) at $q < q_R$ to a dilational-like dispersion ($\Delta\omega \sim q^{1.4}$) for $q > q_R$, without the need of negative values of κ.

Although strictly speaking in Buzza et al.'s[31] model the coupling arises from the bending mode, only expected for a thick monolayer, there are some other possible explanations for the coupling.

Very recently,[29] it has been suggested for fatty acid monolayers that the origin of the negative κ values is the vicinity to a phase transition. These authors suggest that near to the critical point, the surface waves may induce a stripe-like concentration pattern. In addition, both experimental[6,9] and theoretical[2] results of the melting transition of *n*-alcohols show that second-order-like character appears in this transition on decreasing *n* from 16 to 10. Thus, we may argue that this effect may be a plausible explanation for the extra hydrodynamic coupling between the surface modes found in this work for a monolayer of 1-dodecanol.

Also very recently,[55] in a theoretical work on the dilational viscosity of Langmuir monolayers it has been suggested that the orientational effect of the dilational wave on the surface molecules should be considered. This microscopic model might be the basis of a more adequate dispersion equation. Further theoretical and experimental work is needed in order to clarify this point.

Effect of Adsorption Kinetics on the Elasticity. The values obtained for the elasticity $\epsilon(\omega)$ deserve further comments since they are in apparent conflict with recent results reported by Zakri et al.,[9] on the equilibrium thermoelastic behavior of a system similar to the one considered here. It seems to be also in disagreement with the KTHNY theory for 2D freezing[38] which predicts a strong increase of the dilational modulus at $T < T_f$ due to the shear component.

From X-ray Bragg diffraction line broadening measurements performed on 1-decanol monolayers in equilibrium with a reservoir drop, a value of the total dilational modulus, $\epsilon \approx 2500$ mN m^{-1}, was reported[9] in the solid phase at $T < T_f$. This result is compatible with the static values of the compression modulus, ϵ_{st}, obtained from the $\Pi-A$ isotherms of spread monolayers of longer fully insoluble *n*-alcohols. In particular, values moderately high ($\epsilon_{st} \sim 100$ mN m^{-1}) and nearly temperature independent are found from the liquid branches of the $\Pi-A$ isotherm of 1-octadecanol spread on water.[56] Higher values, ~1000 mN m^{-1}, are obtained from the solid branches of these isotherms. The later states correspond to high-pressure and low-temperature phases, which are thermodynamically equivalent to the solid-state considered in our study at $T < T_f$. Moreover, the static compression modulus of the solid phase depends on temperature with a large and positive thermal coefficient (ϵ_{st} clearly increases with temperature in the solid phase leading to a more rigid solid at low temperature).

We must recall that our values of $\epsilon(\omega)$ are lower than the above equilibrium data (see Figure 8) and do not show any significant change with temperature, even when the phase transition takes place.

A plausible explanation of this issue emerges from the nonequilibrium character of our dynamical results. In fact, if the surface dilation is not sufficiently fast (surface mode with finite frequency, ω), mass transfer between the monolayer and the 3D adjacent phases is now possible. In such a situation, the modulation in surface pressure $\Delta\Pi$ caused by a given dilation ΔA is smaller than at equilibrium, where mass transport does not contribute; this would lead to values of $\epsilon(\omega)$ lower than the static or equilibrium ones, ϵ_{st}. To quantify these effects, different mass transport mechanisms for small deviations from the steady-state equilibrium should be considered.

It is not difficult to show that both surface diffusion and monolayer-drop exchange are fully relaxed at the experi-

(55) Kolevzon, V. *Physica A* **1999**, *271*, 1.
(56) Lawrie, G. A.; Barnes, G. T. *J. Colloid Interface Sci.* **1994**, *162*, 36.

mental frequencies of the present study.[28,57] This is not the case for the diffusive exchange between the monolayer and the *subsurface*. Medium-chain alcohols are slightly soluble in water and a partial amount of the monolayer material can be dissolved in the tridimensional aqueous phase adjacent to the interface, the so-called *subsurface*. The characteristic frequency for this motion is given by[35]

$$\omega_{\mathrm{Dif}} = \frac{D}{2}\left(\frac{\mathrm{d}c}{\mathrm{d}\Gamma}\right)^2$$

where c and Γ are the subsurface and surface concentrations, respectively, and D is the bulk diffusion coefficient. For soluble surfactants, as short-chain alcohols, typical values are $\mathrm{d}c/\mathrm{d}\Gamma \sim 10^5$ cm^{-1} and $D \sim 10^{-6}$ cm^2 s^{-1}, from which one obtains $\omega_{\mathrm{Dif}} \sim 10^4$ Hz. Since the $\mathrm{d}c/\mathrm{d}\Gamma$ ratio is expected to strongly increase for slightly soluble or nearly insoluble surfactants such as dodecanol, hence ω_{D} might clearly be larger than the frequency of the surface modes studied by SQELS. Diffusive exchange between the monolayer and the bulk is then allowed and the dynamic dilational modulus becomes lower than the equilibrium value, or Gibbs elasticity, ϵ_{st}, which will be reached when the surface deformation is faster than the time necessary for diffusive exchange with the bulk, i.e., at $\omega \gg \omega_{\mathrm{Dif}}$. The viscoelastic model developed by Lucassen−Van den Tempel predicts a complex dilational modulus depending on frequency as[35]

$$\tilde{\epsilon}(\omega) = \epsilon(\omega) + i\omega\kappa(\omega) = \epsilon_{\mathrm{st}}\frac{\left(1 + \frac{\omega_{\mathrm{Dif}}}{\omega}\right) + i\frac{\omega_{\mathrm{Dif}}}{\omega}}{1 + 2\left(\frac{\omega_{\mathrm{Dif}}}{\omega}\right) + 2\left(\frac{\omega_{\mathrm{Dif}}}{\omega}\right)^2}$$

From which a ratio $\omega_{\mathrm{Dif}}/\omega \sim 10$ can be estimated from our results for the liquid phase, by considering $\epsilon_{\mathrm{st}} \sim 100$ mN m^{-1} and $\epsilon(\omega) \sim 5$ mN m^{-1}, over the whole frequency range (100 Hz to 50 kHz). It is thus clear that the dynamical modulus observed at a given frequency decreases, going far from the Gibbs limit, as the alcohol becomes more hydrophobic. This behavior correlates well with that qualitatively expected from the Lucassen−Van den Tempel model: since $\mathrm{d}c/\mathrm{d}\Gamma$ increases with hydrophobicity, ω_{Dif} becomes an increasing function of the length of the alcohol, and as a consequence, the Gibbs limit ϵ_{st} of the elastic modulus, $\epsilon(\omega) \leq \epsilon_{\mathrm{st}}$, will be only reached at progressively higher frequencies.

It seems therefore clear that the low values of $\epsilon(\omega)$ observed in our experiments might be compatible with a dynamical viscoelastic behavior governed by a diffusion-driven process corresponding to the slight dissolution of the alcohol in the subsurface.

6. Conclusions

We have studied monolayers of 1-dodecanol at a water−air interface in equilibrium with a drop of bulk dodecanol. Both static and dynamic results show that this monolayer undergoes a condensed liquid−solid phase transition at a temperature $T_{\mathrm{f}} \sim 312$ K. At both sides of the 2D phase transition the equilibrium spreading pressure decreases on increasing temperature, indicating that the dodecanol is in a more ordered array at the monolayer than at the liquid drop. The SQELS spectra can be nicely fitted to a Voigt function, giving maximum frequencies, ω_{c}, and half-widths, $\Delta\omega_{\mathrm{c}}$. These data together with the static surface tension have been used to obtain, in framework of the classical dispersion equation (eq 7), the viscoelastic parameters of the monolayer. We obtained dynamic elasticities, $\epsilon(\omega)$, from 3 to 6 mN m^{-1}, these values are much smaller than the expected static elasticity of condensed or solid phases,[9,56] and also smaller than the dynamic elasticity of Gibbs monolayers of 1-octanol and 1-decanol, in the same frequency range.[24] This result can be explained if the diffusion between the surface and the subsurface is considered within the Lucassen−Van de Tempel model.[35]

An important and unexpected result is the sign of the loss module of the elasticity. In fact we have obtained negative values of the dilational viscosity over the whole temperature and wavevector range. To clarify this point we performed ECW measurements, extending in this way the available frequency range. The experimental results show that most of our high-frequency SQELS data lie in a region where $q \geq q_{\mathrm{R}}$, and that in going from low frequencies (ECW) to the high ones we crossover the resonance condition, $q = q_{\mathrm{R}}$. Within eq 7 the negative values of κ can be understood since $\kappa < 0$ is the only reasonable way in which hydrodynamic mode mixing can be achieved. The mode mixing effect may, qualitatively, explain our experimental results in particular the slopes of damping vs wavevector.

Alternatively the experimental results can be quantitatively explained if an extra hydrodynamic coupling term is included in the dispersion equation, without having to use in this case $\kappa < 0$. We have used a modification of the dispersion equation proposed by Buzza et al.[31] The fit of the experimental results with this equation (eq 13) gives elasticities similar to the ones obtained with eq 7 and coupling constants between 2 and 3×10^{-5} mN. The physical origin of such a coupling is clear in the case of thick monolayers, as the copolymers monolayers of Buzza et al.,[31] unfortunately is not that clear in our case of a monolayer made of small molecules. Although, we may argue following other authors that this coupling may be a consequence of the vicinity to the phase transition,[29] this means that the dilational wave must be able to locally change the concentration giving rise to stripe-like phases and/or molecular orientational effects promoted by the dilational wave as it has been very recently suggested by Kolevzon.[55]

Acknowledgment. This work was supported in part by Fundación Ramón Areces, and by DGES under grant PB96-609. F.M. gratefully acknowledge financial support from the Spanish Ministry of Education.

LA0001474

(57) Dukhin, S. S.; Kretzschmar, G.; Miller, R. *Dynamics of Adsorption at Liquids Interfaces*; Elsevier: Amsterdam, 1995; Vol. 1.